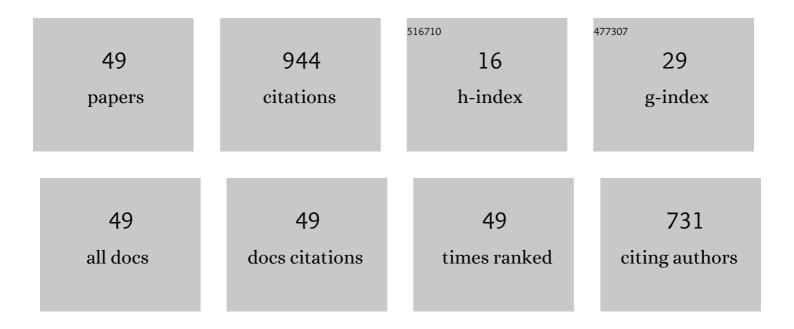
Yao Guo

List of Publications by Year in descending order

Source: https://exaly.com/author-pdf/4294064/publications.pdf Version: 2024-02-01



VAO CUO

#	Article	IF	CITATIONS
1	Regulative Electronic States around Ruthenium/Ruthenium Disulphide Heterointerfaces for Efficient Water Splitting in Acidic Media. Angewandte Chemie - International Edition, 2021, 60, 12328-12334.	13.8	161
2	LiM ^{II} (IO ₃) ₃ (M ^{II} =Zn and Cd): Two Promising Nonlinear Optical Crystals Derived from a Tunable Structure Model of α‣iIO ₃ . Angewandte Chemie - International Edition, 2019, 58, 17194-17198.	13.8	69
3	Broadband white-light emission in a one-dimensional organic–inorganic hybrid cadmium chloride with face-sharing CdCl ₆ octahedral chains. Journal of Materials Chemistry C, 2021, 9, 88-94.	5.5	54
4	LiM ^{II} (IO ₃) ₃ (M ^{II} =Zn and Cd): Two Promising Nonlinear Optical Crystals Derived from a Tunable Structure Model of α‣iIO ₃ . Angewandte Chemie, 2019, 131, 17354-17358.	2.0	49
5	Two Phosphates: Noncentrosymmetric Cs ₆ Mg ₆ (PO ₃) ₁₈ and Centrosymmetric Cs ₂ MgZn ₂ (P ₂ O ₇) ₂ . Inorganic Chemistry, 2017. 56. 845-851.	4.0	48
6	Regulative Electronic States around Ruthenium/Ruthenium Disulphide Heterointerfaces for Efficient Water Splitting in Acidic Media. Angewandte Chemie, 2021, 133, 12436-12442.	2.0	42
7	Effects of Rb Incorporation and Water Degradation on the Stability of the Cubic Formamidinium Lead Iodide Perovskite Surface: A First-Principles Study. Journal of Physical Chemistry C, 2017, 121, 12711-12717.	3.1	40
8	Precise and Wide-Ranged Band-Gap Tuning of Ti ₆ -Core-Based Titanium Oxo Clusters by the Type and Number of Chromophore Ligands. Inorganic Chemistry, 2019, 58, 16785-16791.	4.0	39
9	Metal-organic frameworks derived RuP2 with yolk-shell structure and efficient performance for hydrogen evolution reaction in both acidic and alkaline media. Applied Catalysis B: Environmental, 2022, 305, 121043.	20.2	37
10	Efficient hydrogen generation of vector Z-scheme CaTiO3/Cu/TiO2 photocatalyst assisted by cocatalyst Cu nanoparticles. Journal of Colloid and Interface Science, 2022, 605, 373-384.	9.4	34
11	Highly efficient self-trapped exciton emission in a one-dimensional face-shared hybrid lead bromide. Chemical Communications, 2021, 57, 2495-2498.	4.1	29
12	Pb@Pb ₈ Basket-like-Cluster-Based Lead Tellurate–Nitrate Kleinman-Forbidden Nonlinear-Optical Crystal: Pb ₉ Te ₂ O ₁₃ (OH)(NO ₃) ₃ . Inorganic Chemistry, 2017, 56, 7900-7906.	4.0	26
13	A series of silver doped butterfly-like Ti ₈ Ag ₂ clusters with two Ag ions panelled on a Ti ₈ surface. Dalton Transactions, 2019, 48, 13423-13429.	3.3	26
14	Highly efficient and low hysteresis methylammonium-free perovskite solar cells based on multifunctional oteracil potassium interface modification. Chemical Engineering Journal, 2022, 439, 135671.	12.7	26
15	Tris (8-Hydroxyquinoline) Aluminium Nanostructure Film and Its Fluorescence Properties. Chinese Physics Letters, 2008, 25, 4428-4430.	3.3	18
16	Constructing a full-space internal electric field in a hematite photoanode to facilitate photogenerated-carrier separation and transfer. Journal of Materials Chemistry A, 2022, 10, 8546-8555.	10.3	17
17	KBi(IO ₃) ₃ (OH) and NaBi(IO ₃) ₄ : from the centrosymmetric chain to a noncentrosymmetric double layer. Dalton Transactions, 2019, 48, 10320-10326.	3.3	15
18	Synergetic Influence of Alkali-Metal and Lone-Pair Cations on Frameworks of Tellurites. Inorganic Chemistry, 2018, 57, 5406-5412.	4.0	13

Yao Guo

#	Article	IF	CITATIONS
19	Effects of Transition Metal Substituents on Interfacial and Electronic Structure of CH3NH3PbI3/TiO2 Interface: A First-Principles Comparative Study. Nanomaterials, 2019, 9, 966.	4.1	13
20	Few-Layer MoS ₂ Nanosheet/Carbon Nanotube Composite Films for Long-Lifetime Lithium Storage and Hydrogen Generation. ACS Applied Nano Materials, 2021, 4, 4754-4762.	5.0	13
21	Reconstructing Oxygen Vacancies in the Bulk and Nickel Oxyhydroxide Overlayer to Promote the Hematite Photoanode for Photoelectrochemical Water Oxidation. ACS Applied Energy Materials, 2022, 5, 8999-9008.	5.1	13
22	Structural and electronic characterization of GaN on MgAl ₂ O ₄ (111) substrates. Physica Status Solidi (B): Basic Research, 2016, 253, 1715-1720.	1.5	11
23	Two-Dimensional (001) LaAlO ₃ /SrTiO ₃ Heterostructures with Adjustable Band Gap and Magnetic Properties. ACS Applied Materials & Interfaces, 2020, 12, 3134-3139.	8.0	11
24	Structural, Electronic, and Optical Characterizations of the Interface between CH ₃ NH ₃ PbI ₃ and BaSnO ₃ Perovskite: A First-Principles Study. Journal of Physical Chemistry C, 2019, 123, 16075-16082.	3.1	10
25	Electronic Properties of the Graphdiyne/CH 3 NH 3 PbI 3 Interface: A Firstâ€Principles Study. Physica Status Solidi - Rapid Research Letters, 2020, 14, 1900544.	2.4	10
26	Sr2Pb(BeB5O10)(BO3): An Excellent Ultraviolet Nonlinear-Optical Beryllium Borate by the Pb-Modified Construction of a Conjugated System and Lone-Pair Effect. Inorganic Chemistry, 2021, 60, 11214-11221.	4.0	10
27	Lead Tellurite Crystals BaPbTe ₂ O ₆ and PbVTeO ₅ F with Large Nonlinear-/Linear-Optical Responses due to Active Lone Pairs and Distorted Octahedra. Inorganic Chemistry, 2022, 61, 1538-1545.	4.0	10
28	BeO ₆ Trigonal Prism with Ultralong Be–O Bonds Observed in a Deep Ultraviolet Optical Crystal Li ₁₃ BeBe ₆ B ₉ O ₂₇ . Inorganic Chemistry, 2019, 58, 2201-2207.	4.0	9
29	Interfacial interactions and properties of lead oxysalts passivated MAPbI3 perovskites from first-principles calculations. Computational Materials Science, 2021, 187, 110081.	3.0	9
30	Structural characterization and property modification for two-dimensional (001) SrTiO3 nanosheets. Applied Nanoscience (Switzerland), 2020, 10, 4273-4279.	3.1	8
31	High Coordinate Metal Iodate Chlorides with Diverse Structural Motifs and Tunable Birefringence. Crystal Growth and Design, 2020, 20, 5473-5483.	3.0	8
32	Li6Na3Sr14Al11P22O90: an oxo-centered Al3cluster based phosphate constructed from two types of (3,6)-connected kgd layers. Dalton Transactions, 2018, 47, 298-301.	3.3	7
33	M ₄ LiBe ₄ P ₇ O ₂₄ and M ₄ Li(Li ₃ P)P ₇ O ₂₄ (M = Cs, Rb): deep-ultraviolet nonlinear-optical phosphates with a tetrahedra-substituted paracelsian-like framework. Chemical Communications. 2020. 56. 8639-8642.	4.1	7
34	BaLiTe ₂ O ₅ X (X = Cl, Br): mixed alkali/alkaline-earth metal tellurite halides with [Te ₂ O ₅] _{â~ž} chains. Dalton Transactions, 2020, 49, 4914-4919.	3.3	7
35	Interfacial interactions and enhanced optoelectronic properties of GaN/perovskite heterostructures: insight from first-principles calculations. Journal of Materials Science, 2021, 56, 11352-11363.	3.7	7
36	Theoretical study of the initial stage of InN growth on cubic zirconia (111) substrates. Physica Status Solidi - Rapid Research Letters, 2013, 7, 207-210.	2.4	6

Yao Guo

#	Article	IF	CITATIONS
37	Functionalization of two-dimensional PbTiO3 film by surface modification: A first-principles study. Applied Surface Science, 2021, 563, 150268.	6.1	5
38	First-principles insight into the interfacial properties of epitaxial Bi2O2X (X = S, Se, Te) on SrTiO3 substrates. Journal of Physics and Chemistry of Solids, 2022, 163, 110601.	4.0	5
39	Theoretical Investigation of the Polarity Determination for <i>c</i> -Plane InN Grown on Yttria-Stabilized Zirconia (111) Substrates with Yttrium Surface Segregation. Applied Physics Express, 2013, 6, 021002.	2.4	4
40	The effect of oxygen vacancies on the properties of polar and nonpolar (0 0 1) LaAlO3/SrTiO3 heterostructures. Applied Surface Science, 2018, 450, 260-264.	6.1	4
41	First-principles study of Cs/Rb co-doped FAPbl ₃ stability and degradation in the presence of water and oxygen. Materials Research Express, 2018, 5, 026203.	1.6	4
42	Insights into varying dimension structures for deep-UV optical crystals NaBa2Al(P2O7)2 and NaBaAl(PO4)2 constructed separately from unique [Al(P2O7)2] chains and [Al(PO4)2] layers. Journal of Solid State Chemistry, 2021, 301, 122333.	2.9	4
43	Ca-cluster-constructed deep-ultraviolet nonlinear-optical crystal Na2Ca17Al2(PO4)14 with strong NLO response. Journal of Alloys and Compounds, 2022, 896, 162975.	5.5	2
44	Theoretical Investigation on Structural and Electronic Properties of InN Growth on Ce-Stabilized Zirconia (111) Substrates. Advances in Condensed Matter Physics, 2016, 2016, 1-7.	1.1	1
45	Ab initiocalculations on the initial stages of GaN and ZnO growth on lattice-matched ScAlMgO4(0001) substrates. Materials Research Express, 2016, 3, 125903.	1.6	1
46	First-principles study of the atomic and electronic properties of (1 0 0) stacking faults in BaSnO3 crystal. Chemical Physics Letters, 2018, 694, 65-69.	2.6	1
47	Design and synthesis of PbBiVO5 electrode by polymorph engineering for rechargeable battery. Journal of Solid State Chemistry, 2021, 293, 121777.	2.9	1
48	Theoretical study of InN growth on Mn-stabilized zirconia (111) substrates. Thin Solid Films, 2014, 551, 110-113.	1.8	0
49	Comparative studies of wurtzite and zincblende indium nitride/yttria-stabilized zirconia interfacial and electronic properties by first-principles calculations. Japanese Journal of Applied Physics, 2018, 57, 100304.	1.5	0